



CHORUS

This is the accepted manuscript made available via CHORUS. The article has been published as:

Robust Majorana Conductance Peaks for a Superconducting Lead

Yang Peng, Falko Pientka, Yuval Vinkler-Aviv, Leonid I. Glazman, and Felix von Oppen
Phys. Rev. Lett. **115**, 266804 — Published 29 December 2015

DOI: [10.1103/PhysRevLett.115.266804](https://doi.org/10.1103/PhysRevLett.115.266804)

Robust Majorana conductance peaks for a superconducting lead

Yang Peng,¹ Falko Pientka,¹ Yuval Vinkler-Aviv,¹ Leonid I. Glazman,² and Felix von Oppen¹

¹*Dahlem Center for Complex Quantum Systems and Fachbereich Physik, Freie Universität Berlin, 14195 Berlin, Germany*

²*Department of Physics, Yale University, New Haven, CT 06520, USA*

Experimental evidence for Majorana bound states largely relies on measurements of the tunneling conductance. While the conductance into a Majorana state is in principle quantized to $2e^2/h$, observation of this quantization has been elusive, presumably due to temperature broadening in the normal-metal lead. Here, we propose to use a superconducting lead instead, whose gap strongly suppresses thermal excitations. For a wide range of tunneling strengths and temperatures, a Majorana state is then signaled by symmetric conductance peaks at $eV = \pm\Delta$ of a universal height $G = (4 - \pi)2e^2/h$. For a superconducting scanning tunneling microscope tip, Majorana states appear as spatial conductance plateaus while the conductance varies with the local wavefunction for trivial Andreev bound states. We discuss effects of nonresonant (bulk) Andreev reflections and quasiparticle poisoning.

Introduction.—Motivated by possible applications in quantum information processing [1, 2], topological superconductors hosting Majorana bound states are currently under intense investigation [3–5]. Based on the superconducting proximity effect, various realistic platforms have been proposed to support Majorana states including topological insulators [6, 7], semiconductor nanowires [8, 9], and atomic chains [10–16]. Although these systems are available in the laboratory, the experimental observation of unique Majorana signatures remains challenging.

A widely employed diagnostic tool is the tunneling conductance of normal metal–superconductor junctions, in which Majoranas manifest themselves as characteristic zero-bias peaks [17, 18]. Experimental signatures consistent with theoretical predictions have been observed in quantum wires [20–22] and atomic chains [23, 24]. However, it is a major challenge in these experiments to uniquely distinguish Majoranas from conventional fermionic subgap states. Spin-polarized subgap states such as Shiba states bound to magnetic impurities [25–28] or Andreev bound states in a magnetic field can exhibit a zero-energy crossing as a function of exchange interaction or Zeeman energy [29–31]. Thus, such fermionic states may accidentally occur at zero energy and give rise to similar conductance features. As magnetic impurities or external magnetic fields are also required for the most relevant realizations of topological superconductors, such trivial conductance peaks can generally not be disregarded.

In contrast to fermionic subgap states, Majoranas exhibit a celebrated quantized zero-bias conductance of $2e^2/h$ [17–19]. Unfortunately, this has so far proved difficult to observe in experiment. The Fermi distribution in the metal lead is smooth on the scale of the temperature T , which strongly limits the experimental energy resolution. When temperature is larger than the tunnel coupling, the Majorana peak is broadened and the zero-bias conductance is reduced. Even at low temperatures (e.g., $T = 60$ mK in Ref. [20]), it may be difficult to observe the quantized peak height as multichannel effects

limit the relevant tunneling strength [32]. Quasiparticle poisoning may also lead to deviations from quantization. A fermion-parity breaking rate exceeding the tunnel coupling broadens the peak and reduces its height. This requires one to work at temperatures below the lowest fermionic excitations in the topological superconductor.

In this paper, we show how a robust conductance signature of Majorana bound states can be obtained by employing superconducting leads. In striking contrast to normal-state contacts, effects of thermal broadening are strongly suppressed for a superconducting lead because quasiparticle excitations are exponentially suppressed $\sim \exp(-\Delta/T)$ by its superconducting gap Δ . Majorana bound states no longer appear as zero-bias anomalies but rather as two symmetric peaks in the differential conductance $G = dI/dV$ which occur when the BCS singularity of the superconducting gap lines up with the Majorana bound state, i.e., at the thresholds $eV = \pm\Delta$. These peaks have a universal height

$$G_M = (4 - \pi) \frac{2e^2}{h}, \quad (1)$$

which persists over a wide range of tunnel couplings.

This yields particularly striking evidence when employing a scanning tunneling microscope (STM) with a superconducting tip which allows for spatially resolved measurements. This has previously been used to map out bound state wavefunctions in conventional and unconventional superconductors [23, 24, 33–36]. Here we propose that such maps can clearly distinguish between Majoranas and trivial zero-energy bound states. Indeed, the peak conductance is uniform in the vicinity of Majorana states and a conductance map exhibits a characteristic mesa or plateau structure. In contrast, the conductance of trivial subgap states exhibits a spatial pattern which is governed by the bound-state wavefunction.

In addition, STM measurements allow for systematic studies as a function of tunneling strength by varying the tip height. It was recently demonstrated [37] that this can be exploited to probe quasiparticle relaxation

processes. In the present context, varying the tunneling strength may help to identify Majorana signatures despite competing effects such as nonresonant Andreev reflections or quasiparticle poisoning.

Subgap conductance for Majorana bound state.—At subgap voltages $eV < \Delta + \Delta_s$ and zero temperature, the tunneling current between superconducting tip or lead and substrate (with gap Δ_s) flows by multiple Andreev reflections. Near the threshold $e|V| = \Delta$, the differential conductance dI/dV is dominated by single Andreev reflections from the sample. For tip locations far from the zero-energy bound state in the sample, this yields the familiar peak in dI/dV due to the singular densities of states of incoming electrons and outgoing holes. In the vicinity of the bound state, tunneling is further enhanced by the zero-energy resonance [37–39].

Formally, the subgap current due to single Andreev reflections from the sample can be expressed as [40–42]

$$I(V) = 4e\pi^2 t^4 \int \frac{d\omega}{2\pi\hbar} \text{Tr}[G_{eh}(r, \omega) G_{eh}^\dagger(r, \omega)] \times \rho(\omega_-) \rho(\omega_+) [n_F(\omega_-) - n_F(\omega_+)], \quad (2)$$

where t is the amplitude for tip-substrate tunneling, $\omega_\pm = \omega \pm eV$, $n_F(\omega)$ denotes the Fermi function, and the superconducting tip enters through its BCS density of states $\rho(\omega) = \nu_0 \theta(|\omega| - \Delta) |\omega| / \sqrt{\omega^2 - \Delta^2}$ with ν_0 the normal density of states at the Fermi energy. Spin or subband degrees of freedom are accounted for by a possible matrix structure of the anomalous retarded Green function $G_{eh}(r, \omega)$ of the substrate at the tip position r . In terms of its Lehmann representation, $G_{eh}(r, \omega)$ has contributions from both the bound state and the above-gap continuum. In the following, we first consider the resonantly enhanced Andreev current from a Majorana bound state and subsequently discuss the contribution of the quasiparticle continuum.

For $e|V| \simeq \Delta$, we can approximate $n_F(\omega_-) - n_F(\omega_+) \simeq \text{sgn}V$ in Eq. (2), up to corrections of order $\exp(-\Delta/T)$. This insensitivity to temperature is a key advantage of superconducting leads. The bound-state contribution to the substrate Green function is

$$G(r, \omega) = \frac{\langle r|\psi\rangle\langle\psi|r\rangle}{\omega + i\Gamma/2}. \quad (3)$$

Here, $\langle r|\psi\rangle = [\zeta(r), \pm\Theta\zeta(r)]^T$ denotes the local Bogoliubov–de Gennes wavefunction of the Majorana bound state with Θ the time-reversal operator. The broadening $\Gamma = 2i\langle\psi|\Sigma|\psi\rangle$ of the bound state is induced by the tunnel coupling to the lead. The corresponding self energy $\Sigma = -i\pi t^2 \text{diag}[\rho(\omega_-), \rho(\omega_+)]$ is diagonal as Andreev reflections in the lead can be neglected near $e|V| = \Delta$.

Inserting Eq. (3) into (2) yields (for $V > 0$) [37, 43]

$$I = \frac{e}{h} \int d\omega \frac{\Gamma_e(\omega)\Gamma_h(\omega)}{\omega^2 + [\Gamma_e(\omega) + \Gamma_h(\omega)]^2/4} \quad (4)$$

in terms of the electron and hole tunneling rates $\Gamma_{e/h}(\omega) = 2\pi t^2 |\zeta|^2 \rho(\omega_\mp)$. While the integrand in Eq. (4) has a resonance denominator, its behavior is peculiar due to the strong energy dependence of the tunneling rates. Specifically, the square-root singularity of the BCS density of states implies that the integrand involves a characteristic energy scale $\omega_t = (\pi t^2 \nu_0 |\zeta(r)|^2 \sqrt{\Delta/2})^{2/3}$ which depends on a fractional power of the tunneling rate from a normal tip $\gamma_n = 2\pi t^2 \nu_0 |\zeta(r)|^2$. In the weak-tunneling regime $\omega_t \ll \Delta$, we can write

$$I = \frac{4e}{h} \int_{-\eta}^{\eta} \frac{d\omega}{\sqrt{\eta^2 - \omega^2}} \frac{\omega_t^3}{\omega^2 + \omega_t^3 \left(\frac{1}{\sqrt{\eta - \omega}} + \frac{1}{\sqrt{\eta + \omega}} \right)^2}, \quad (5)$$

for $0 < \eta \ll \Delta$, where $\eta = eV - \Delta$ measures the voltage from the threshold Δ . In the vicinity of the threshold, $\eta \ll \omega_t$, the resonance denominator is dominated by the second term and we obtain $I(V) = (4 - \pi)(2e/h)(eV - \Delta)\theta(eV - \Delta)$ and thus Eq. (1). The entire peak lineshape

$$\frac{dI}{dV} = (4 - \pi) \frac{2e}{h} \Lambda\left(\frac{eV - \Delta}{\omega_t}\right), \quad (6)$$

involves the function $\Lambda(x)$ which vanishes for $x < 0$, jumps to $\Lambda(0^+) = 1$, and falls off with a small negative differential conductance tail at large x , cp. Fig. 1.

Thus, the differential conductance between a conventional superconductor and a Majorana state exhibits a peak which is independent of tunneling strength and Majorana wavefunction. While the peak height is close to the quantized Majorana peak height $2e^2/h$ for a normal-metal lead, there are several differences: (a) There are two symmetric, finite-bias Majorana peaks at $eV = \pm\Delta$ rather than a single zero-bias peak, (b) the conductance peak is strongly asymmetric with a discontinuous step at the threshold, and (c) the width of the peak is set by ω_t with its sublinear dependence on junction transparency.

The threshold discontinuity in the conductance persists even when including the contributions of the quasiparticle continuum in the substrate Green function. To see this, we model the substrate superconductor by a 2×2 Nambu Green function $g(\omega, r)$. For a topological substrate, this is appropriate for perfect spin polarization (spinless p -wave superconductor). Including the tunnel coupling to the tip through the self energy Σ as given above, the substrate Green function becomes $G = g[1 - \Sigma g]^{-1}$. We first focus on the vicinity of the bound state where the conductance is dominated by Andreev reflections from the bound state. By straightforward calculation and expansion of g in ω [40], we find

$$G(r, \omega) = \frac{\langle r|\psi\rangle\langle\psi|r\rangle}{\omega - \lambda(\omega) + i\Gamma/2}. \quad (7)$$

This differs from the pure bound-state contribution by the additional term $\lambda(\omega) = \pi^2 t^4 \omega \det g(\omega, r) \rho(\omega_-) \rho(\omega_+)$ in the denominator which involves the determinant (in

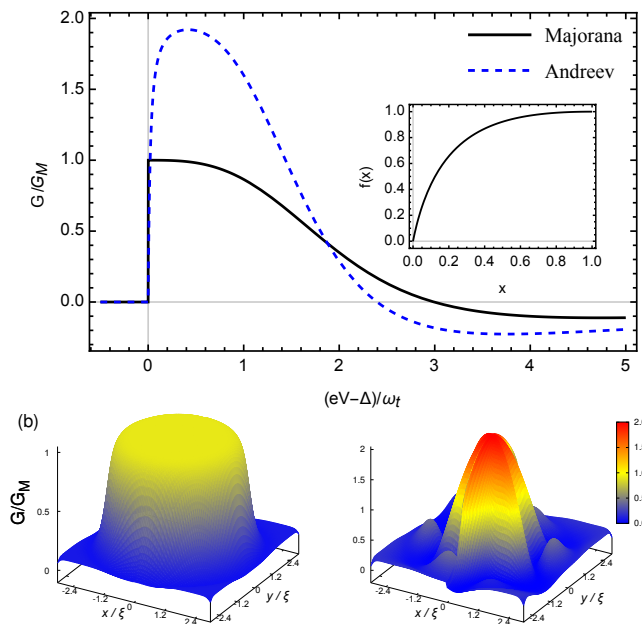


FIG. 1. (color online) (a) Differential conductance *vs* bias voltage near the threshold $eV = \Delta$ for Majorana (solid line) and Andreev state with $|u| = |v|$ (dashed line). For a Majorana, the conductance exhibits a step of height $(4 - \pi)2e^2/h$ at the threshold. For an Andreev state, the conductance has a smooth onset, cf. Eq. (10). Both peaks have a negative-differential conductance dip at high voltages. Inset: Graph of $f(x)$ as defined in the main text. (b) Spatial conductance maps for Majorana (left) and Andreev state (right) for $\omega_t(0)/\delta\Delta = 5$. The Majorana gives rise to a conductance plateau whereas the Andreev state exhibits a pattern reflecting the spatial dependence of the ratio $(u/v)^2$. The Majorana conductance drops far from the bound state when the broadening exceeds ω_t .

particle-hole space) of the bare substrate Green function. While the determinant of the bound-state contribution to the Green function vanishes, this is no longer the case when including the quasiparticle continuum. At subgap energies away from bound states, the Green function $g(\omega, r)$ is a hermitian 2×2 matrix, so that $\det g(\omega, r)$ and hence $\lambda(\omega)$ are real. Thus, we find

$$I_M(V) = \frac{4e}{h} \int_{-\eta}^{\eta} \frac{d\omega}{\sqrt{\eta^2 - \omega^2}} \frac{\omega_t^3}{(\omega - \lambda)^2 + \left(\frac{\omega_t^{3/2}}{\sqrt{\eta - \omega}} + \frac{\omega_t^{3/2}}{\sqrt{\eta + \omega}}\right)^2}. \quad (8)$$

For a Majorana state, the real part of the resonance denominator must vanish exactly at $\omega = 0$. Indeed, particle-hole symmetry further constrains $\det g(\omega, r)$ to be an even function of ω which can be approximated as a constant at small ω (see [40], where this conclusion is confirmed by model calculations). Then, we find $\lambda(\omega) \propto t^4 \omega / \sqrt{\eta^2 - \omega^2}$ near the threshold. Even with this term, the denominator in Eq. (8) remains dominated by the divergent tunnel broadenings $\sim \omega_t^{3/2} / \sqrt{\eta \pm \omega}$ and the

discontinuous conductance step as well as the universal value of the threshold conductance in Eq. (1) persist.

In experiment, the square-root singularity of the BCS density of states of the tip may be broadened intrinsically due to higher-order processes or effectively due to experimental resolution. The universal threshold conductance persists as long as ω_t exceeds this broadening. This condition also determines the spatial extent of the conductance plateau, $r \lesssim 4\xi \ln[\omega_t(0)/\delta\Delta]/3$, where ξ is the Majorana localization length, $\omega_t(0)$ denotes the value of ω_t at the center of the Majorana bound state, and $\delta\Delta$ is the broadening of the tip density of state, cf. Fig. 1(b). Of course, a well-resolved Majorana peak also requires $\omega_t \ll \Delta_s$, i.e., the tunnel broadening needs to be small compared to the induced gap. If the peak is not fully resolved, it is suppressed below the universal value and its height may vary as a function of space.

For tip locations far from the bound state, the tunneling conductance is dominated by conventional (“nonresonant”) Andreev reflections. These still yield a threshold peak due to the singular tip density of states in Γ_e and Γ_h , but are not enhanced by a bound-state resonance. For a one-dimensional p -wave superconductor, this conductance peak has height $\simeq 1.3G_M$ and width $\sim \Delta\mathcal{T}^2$ quadratic in the junction transparency $\mathcal{T} \propto t^2$ [40]. Observing the conventional Andreev peak thus requires that the broadening of the tip density of states is small compared to $\sim \Delta\mathcal{T}^2$. This is a much more stringent condition than for the resonant Andreev peak as the width of the bound-state peak $\omega_t \propto t^{4/3}$ involves a lower power of t . We note that in a typical STM experiment [37], conventional Andreev peaks can be resolved only for small tip-sample distances, while bound-state signatures persist to much weaker tunnel couplings.

Subgap conductance for Andreev bound state.—These results should be contrasted with those for trivial zero-energy Andreev bound states. For concreteness, consider an s -wave superconductor with conserved spin [44], whose Bogoliubov–de Gennes description decomposes into two independent spin sectors that interchange under particle-hole transformations. A zero-energy Andreev state corresponds to two Bogoliubov–de Gennes wavefunctions, $\langle r|\psi_+\rangle = [u(r), v(r)]^T$ and $\langle r|\psi_-\rangle = [\Theta v(r), -\Theta u(r)]^T$, one in each sector. An analogous calculation [40] yields the threshold current

$$I_A(V) = 2I_M(V)f(|u(r)|^2/|v(r)|^2). \quad (9)$$

Reflecting the two zero-energy wavefunctions, the maximal threshold conductance is twice that in the Majorana case, $G_A = 2G_M$, and realized for the particle-hole symmetric case $|u| = |v|$. In general, the peak conductance depends on the ratio of electron and hole wavefunction at the tip position. This dependence is captured by the dimensionless function $f(x) = \frac{2x}{4-\pi} \int_{-1}^1 dz \sqrt{1-z^2} / (x\sqrt{1-z} + \sqrt{1+z})^2$ which takes on

values between 0 and 1 and is plotted in Fig. 1(a). The function satisfies $f(x) = f(1/x)$ as the two spin sectors contribute equally. In the limit of large particle-hole asymmetry, $G_A \sim G_M \min(|u/v|^2, |v/u|^2) \ll G_M$. The lineshape of the conductance peak is similar to the Majorana peak, with a width of order ω_t upon replacing $\zeta(r)$ by $\max\{u(r), v(r)\}$.

Our results imply that the height of the conductance peak allows for a clear distinction between a conventional Andreev bound state and a Majorana state. Even when $f(u^2/v^2) \sim 1/2$ for one location of the STM tip, moving the tip to another location modifies the conductance peak height for a conventional bound state, tracking the ratio of electron and hole wavefunctions. In contrast, the conductance map exhibits a characteristic mesa structure for a Majorana state, see Fig. 1(b). In non-STM tunneling experiments, changes of parameters (e.g., gate voltages) which affect the Majorana wavefunction should leave the peak height unchanged for a Majorana but not for a conventional Andreev bound state.

As there is no locking of the bound state to zero energy, also the continuum contribution is distinctly different for conventional Andreev states. The two spin sectors are described by separate 2×2 Nambu Green functions which map into one another under particle-hole transformations. This is quite unlike the Majorana Green function which maps onto itself. For each sector, $\det g(\omega, r)$ is therefore no longer an even function of ω and will generally have a singular contribution $\propto 1/\omega$ at the threshold so that $\lambda(\omega) \sim \mathcal{T}^2 \Delta_s \Delta / \sqrt{\eta^2 - \omega^2}$. These general arguments can be confirmed explicitly for Shiba states in s -wave superconductors [40]. Near the threshold, the resonance denominator in the expression for the current is now dominated by $\lambda(\omega)$. As illustrated in Fig. 1 by a numerical evaluation of the current, this suppresses the conductance step. Analytically, we find that just above the threshold, the conductance increases linearly,

$$G_A(V) \sim \frac{2e^2}{h} \frac{1}{\mathcal{T}^2} \frac{eV - \Delta}{\Delta} \theta(eV - \Delta), \quad (10)$$

and matches with the conductance obtained from Eq. (9) for $eV - \Delta \gg \mathcal{T}^2 \Delta$. We note that this suppression of the conductance step depends on \mathcal{T} and can thus be probed by varying the tip-sample distance in an STM experiment. This may serve as an additional signature to distinguish between Majorana and conventional Andreev bound states.

Effects of quasiparticle poisoning.—So far, we only included bound-state broadening by the tunneling contact. At finite temperatures, the bound-state occupation also changes by inelastic transitions to other subgap states or the quasiparticle continuum in the sample [45]. We account for these processes by an additional contribution $i\Gamma_{qp}/2$ to the self energy of the bound-state Green function Eq. (7). This does not affect the Andreev current at the threshold, where the denominator is dominated

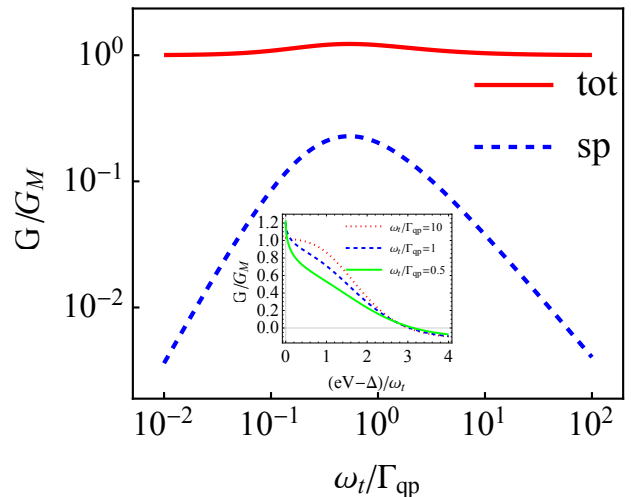


FIG. 2. Total threshold conductance for a Majorana state (tot) along with the single-particle contribution (sp) as a function of ω_t . The single-particle contribution affects the conductance only in a window of transmission values, where $\omega_t \sim \Gamma_{qp}$. While the maximum is of order $0.2G_M$, the position of the maximum in tunneling strength depends sensitively on temperature (through Γ_{qp}). Inset: Line shape of the total conductance as a function of voltage away from the threshold, for different ratios of ω_t/Γ_{qp} .

by the diverging tunnel coupling. However, the overall weight of the peak is reduced by a *narrowing* of the linewidth by a factor $(\omega_t/\Gamma_{qp})^2$ once $\Gamma_{qp} > \omega_t$, see Fig. 2 (inset).

In addition, quasiparticle poisoning generates a single-electron current I^s which involves tunneling of single particles followed by inelastic transitions from the zero-energy bound state to other bound states or the quasiparticle continuum [37]. For a Majorana state, we find near the threshold $eV = \Delta$ (with analogous results applying for Andreev bound states) [40]

$$I_M^s = \frac{e}{4h} \int d\omega \frac{\Gamma_{qp}[\Gamma_e(\omega) + \Gamma_h(\omega)]}{\omega^2 + [\Gamma_{qp} + \Gamma_e(\omega) + \Gamma_h(\omega)]^2/4}. \quad (11)$$

For weak and strong tunneling, this yields [40]

$$G_M^s \sim \frac{2e^2}{h} \begin{cases} (\omega_t/\Gamma_{qp})^{3/2} & \omega_t \ll \Gamma_{qp}, \\ \Gamma_{qp}/\omega_t & \omega_t \gg \Gamma_{qp}. \end{cases} \quad (12)$$

Figure 2 shows that this single-particle contribution assumes a maximum of $\sim 0.2G_M$ when $\omega_t \sim \Gamma_{qp}$. However, it can be easily made negligible by tuning the system away from this maximum through varying temperature or tunneling strength.

Conclusions.—We show that conductance measurements with superconducting leads constitute a promising technique to identify Majorana states. The presence of Majoranas is signaled by conductance peaks of universal height which are largely unaffected by thermal broadening, a key obstacle in previous experiments with normal-metal contacts. We discuss strategies to systematically

rule out parasitic effects such as quasiparticle poisoning or trivial subgap states. The proposed setup is readily available in the laboratory and, in fact, has already been realized in previous experiments [23, 24, 46, 47]. (Notice, however, that temperature was comparable to the induced gap in the STM experiments performed to date, precluding observation of the universal conductance, and that the nanowire experiments focused on zero-bias peaks.) Our results also imply that quasiparticle poisoning rates can be extracted from systematic measurements as a function of tip height and temperature.

Acknowledgments.—We thank P. Brouwer, K. Franke, B. Heinrich, J. Meyer, Y. Oreg, and M.-T. Rieder for stimulating discussions. We acknowledge financial support by the Helmholtz Virtual Institute “New states of matter and their excitations,” SFB 658, SPP1285 and SPP1666 of the Deutsche Forschungsgemeinschaft, the Humboldt Foundation, the Minerva Stiftung, as well as DOE contract DE-FG02-08ER46482 at Yale University. We are grateful to the Aspen Center for Physics, supported by NSF Grant No. PHYS-106629, for hospitality while this line of work was initiated.

-
- [1] A. Kitaev, *Ann. Phys.* **303**, 2 (2003).
 [2] C. Nayak, S.H. Simon, A. Stern, M. Freedman, and S. Das Sarma, *Rev. Mod. Phys.* **80**, 1083 (2008).
 [3] J. Alicea, *Rep. Prog. Phys.* **75**, 076501 (2012).
 [4] C.W.J. Beenakker, *Annu. Rev. Con. Mat. Phys.* **4**, 113 (2013).
 [5] S.R. Elliott and M. Franz, *Rev. Mod. Phys.* **87**, 137 (2015).
 [6] L. Fu and C.L. Kane, *Phys. Rev. Lett.* **100**, 096407 (2008).
 [7] L. Fu and C. L. Kane, *Phys. Rev. B* **79**, 161408(R) (2009).
 [8] R.M. Lutchyn, J.D. Sau, and S. Das Sarma, *Phys. Rev. Lett.* **105**, 077001 (2010).
 [9] Y. Oreg, G. Refael, and F. von Oppen, *Phys. Rev. Lett.* **105**, 177002 (2010).
 [10] S. Nadj-Perge, I.K. Drozdov, B.A. Bernevig, and A. Yazdani, *Phys. Rev. B* **88**, 020407(R) (2013).
 [11] B. Braunecker and P. Simon, *Phys. Rev. Lett.* **111**, 147202 (2013).
 [12] M.M. Vazifeh and M. Franz, *Phys. Rev. Lett.* **111**, 206802 (2013).
 [13] J. Klinovaja, P. Stano, A. Yazdani, and D. Loss, *Phys. Rev. Lett.* **111**, 186805 (2013).
 [14] F. Pientka, L.I. Glazman, and F. von Oppen, *Phys. Rev. B* **88**, 155420 (2013).
 [15] Y. Kim, M. Cheng, B. Bauer, R.M. Lutchyn, and S. Das Sarma, *Phys. Rev. B* **90**, 060401(R) (2014).
 [16] Y. Peng, F. Pientka, L.I. Glazman, and F. von Oppen, *Phys. Rev. Lett.* **114**, 106801 (2015).
 [17] K.T. Law, P.A. Lee, T.K. Ng, *Phys. Rev. Lett.* **103**, 237001 (2009).
 [18] K. Flensberg, *Phys. Rev. B* **82**, 180516 (2010).
 [19] M. Wimmer, A.R. Akhmerov, J.P. Dahlhaus, C.W.J. Beenakker, *New J. Phys.* **13**, 053016 (2011).
 [20] V. Mourik, K. Zuo, S.M. Frolov, S.R. Plissard, E.P.A.M. Bakkers, and L.P. Kouwenhoven, *Science* **336**, 1003 (2012).
 [21] A. Das, Y. Ronen, Y. Most, Y. Oreg, M. Heiblum, and H. Shtrikman, *Nature Phys.* **8**, 887 (2012).
 [22] H.O.H. Churchill, V. Fatemi, K. Grove-Rasmussen, M.T. Deng, P. Caroff, H.Q. Xu, and C.M. Marcus, *Phys. Rev. B* **87**, 241401(R) (2013).
 [23] S. Nadj-Perge, I.K. Drozdov, J. Li, H. Chen, S. Jeon, J. Seo, A.H. MacDonald, B.A. Bernevig, A. Yazdani, *Science* **346**, 602 (2014).
 [24] M. Ruby, F. Pientka, Y. Peng, F. von Oppen, B.W. Heinrich, K.J. Franke, *Phys. Rev. Lett.* **115**, 197204 (2015).
 [25] L. Yu, *Acta Phys. Sin.* **21**, 75 (1965).
 [26] H. Shiba, *Prog. Theor. Phys.* **40**, 435 (1968).
 [27] A.I. Rusinov, *Zh. Eksp. Teor. Fiz. Pisma Red.* **9**, 146 (1968) [*JETP Lett.* **9**, 85 (1969)].
 [28] A.V. Balatsky, I. Vekhter, and J.-X. Zhu, *Rev. Mod. Phys.* **78**, 373 (2006).
 [29] K.J. Franke, G. Schulze, and J.I. Pascual, *Science* **332**, 940 (2011).
 [30] R.S. Deacon, Y. Tanaka, A. Oiwa, R. Sakano, K. Yoshida, K. Shibata, K. Hirakawa, and S. Tarucha, *Phys. Rev. Lett.* **104**, 076805 (2010).
 [31] E.J.H. Lee, X. Jiang, M. Houzet, R. Aguado, C.M. Lieber and S. De Franceschi, *Nat. Nano.* **9**, 79 (2014).
 [32] F. Pientka, G. Kells, A. Romito, P.W. Brouwer, F. von Oppen, *Phys. Rev. Lett.* **109**, 227006 (2012).
 [33] A. Yazdani, B.A. Jones, C.P. Lutz, M.F. Crommie, and D.M. Eigler, *Science* **275**, 1767 (1997).
 [34] A. Yazdani, C.M. Howald, C.P. Lutz, A. Kapitulnik, and D.M. Eigler, *Phys. Rev. Lett.* **83**, 176 (1999).
 [35] E.W. Hudson, K.M. Lang, V. Madhavan, S.H. Pan, H. Eisaki, S. Uchida, and J.C. Davis, *Nature (London)* **411**, 920 (2001).
 [36] S.-H. Ji, T. Zhang, Y.-S. Fu, X. Chen, X.-C. Ma, J. Li, W.-H. Duan, J.-F. Jia, and Q.-K. Xue, *Phys. Rev. Lett.* **100**, 226801 (2008).
 [37] M. Ruby, F. Pientka, Y. Peng, F. von Oppen, B.W. Heinrich, K.J. Franke, *Phys. Rev. Lett.* **115**, 087001 (2015).
 [38] D. Badiane, M. Houzet, J.S. Meyer, *Phys. Rev. Lett.* **107**, 177002 (2011).
 [39] P. San-Jose, J. Cayao, E. Prada, R. Aguado, *New. J. Phys.* **15**, 075019 (2013).
 [40] Supplementary Material
 [41] J.C. Cuevas, A. Martín Rodero, and A. Levy Yeyati, *Phys. Rev. B*, **54**, 7366 (1996).
 [42] I. Martin and D. Mozyrsky, *Phys. Rev. B* **90**, 100508 (2014).
 [43] A. Levy Yeyati, J.C. Cuevas, A. López-Dávalos, and A. Martín-Rodero, *Phys. Rev. B* **55**, R6137(R) (1997).
 [44] The conductance of Andreev states in p -wave or spin-orbit coupled superconductors is discussed in [40].
 [45] The importance of quasiparticle poisoning depends strongly on temperature. Recent experiments on proximity-coupled quantum wires [A.P. Higginbotham *et al.*, *Nat. Phys.*, doi:10.1038/nphys3461 (2015)] find time scales as long as 10ms.
 [46] M.T. Deng, C.L. Yu, G.Y. Huang, M. Larsson, P. Caroff, and H.Q. Xu, *Nano Lett.* **12**, 6414 (2012).
 [47] A.D.K. Finck, D.J. Van Harlingen, P.K. Mohseni, K. Jung, and X. Li, *Phys. Rev. Lett.* **110**, 126406 (2013).